Available online at www.sciencedirect.com
ScienceDirect
Ceramics International 36 (2010) 1937–1943
CERAMICS INTERNATIONAL
www.elsevier.com/locate/ceramint

Conductivity and electrochemical performance of $(Ba_{0.5}Sr_{0.5})_{0.8}La_{0.2}CoO_{3-\delta}$ cathode for intermediate-temperature solid oxide fuel cell

I-Ming Hung *, Chen-Yu Liang, Chun-Jing Ciou, Yu-Chen Lee

Yuan Ze Fuel Cell Center, Department of Chemical Engineering and Materials Science, Yuan Ze University, No. 135, Yuan-Tung Road, Chungli, Taoyuan 320, Taiwan

Received 6 November 2009; received in revised form 4 March 2010; accepted 23 March 2010
Available online 29 April 2010

Abstract

This study reports the successful preparation of a single-phase cubic $(Ba_{0.5}Sr_{0.5})_{0.8}La_{0.2}CoO_{3-\delta}$ perovskite by the citrate–EDTA complexing method. Its crystal structure, thermogravimetry, coefficient of thermal expansion, electric conductivity, and electrochemical performance were investigated to determine its suitability as a cathode material for intermediate-temperature solid oxide fuel cells (IT-SOFCs). Its coefficient of thermal expansion shows abnormal expansion at 300 °C, which is associated with the loss of lattice oxygen. The maximum conductivity of a $(Ba_{0.5}Sr_{0.5})_{0.8}La_{0.2}CoO_{3-\delta}$ electrode is 689 S/cm at 300 °C. Above 300 °C, the electronic conductivity of $(Ba_{0.5}Sr_{0.5})_{0.8}La_{0.2}CoO_{3-\delta}$ decreases due to the formation of oxygen vacancies. The charge-transfer resistance and gas phase diffusion resistance of a $(Ba_{0.5}Sr_{0.5})_{0.8}La_{0.2}CoO_{3-\delta}$–$Ce_{0.8}Sm_{0.2}O_{1.9}$ composite cathode are 0.045 Ω cm^2 and 0.28 Ω cm^2, respectively, at 750 °C.

Keywords: A. Powders: chemical preparation; D. Perovskites; Cathode; Ceramics; Conductivity; Solid oxide fuel cell

1. Introduction

Solid oxide fuel cells (SOFCs) have many advantages over traditional fuel cells, such as high-energy conversion efficiency, high power density, environmental friendliness, and flexibility in using fuels [1–4]. Lowering the operation temperature of SOFCs to 600–800 °C, on the basis of the performance of high-conductivity electrolyte materials [5–8], not only widens the choice of possible materials for interconnectors and significantly reduces production and application costs but also improves the SOFC's stability and reliability. However, the conductivity and electrochemical performance of cathode materials decrease significantly at low temperatures. Therefore, it is important to develop new, high-performance cathode materials for intermediate-temperature SOFCs (IT-SOFCs).

Recently, several kinds of perovskite oxides have been used as cathode electrodes for IT-SOFCs [9–11]. $Ba_{0.5}Sr_{0.5}Co_{0.8}Fe_{0.2}O_{3-\delta}$ (BSCF) has good oxygen permeation and an acceptable conductivity and has been used as an oxygen separation membrane [12,13]. Recently, BSCF was applied as a new cathode material for IT-SOFCs by Shao [14]. It exhibited a high power density of 1010 mW/cm^2 at 600 °C when hydrogen was used as fuel and air as the cathode gas. Despite these favorable results, significant problems remain, especially the low electrical conductivity of BSCF, which is nearly one order of magnitude less than that in commonly used cathodes and may limit electron transmission in the cathode. Li reported doped-BSCF perovskite-type oxides with high electrical conductivity, such as $(Ba_{0.5}Sr_{0.5})_{1-x}Sm_xCo_{0.8}Fe_{0.2}O_{3-\delta}$ (BSSCF) [15,16] and $(Ba_{0.5}Sr_{0.5})_{1-x}La_xCo_{0.8}Fe_{0.2}O_{3-\delta}$ (BSLCF) [17]. The maximum conductivities of BSSCF and BSLCF are 85.6 S/cm at 500 °C and 376 S/cm at 392 °C, respectively.

In this study, $(Ba_{0.5}Sr_{0.5})_{0.8}La_{0.2}CoO_{3-\delta}$ (BSLC) was prepared by the citrate–EDTA complexing method, which allows the formation of single-phase perovskite oxide. The crystal structure, lattice oxygen loss, coefficient of thermal expansion, electrical conductivity, and electrochemical performance of BSLC were investigated.

* Corresponding author. Tel.: +886 3 4638800x2569; fax: +886 3 4630634.
E-mail address: imhung@saturn.yzu.edu.tw (I.-M. Hung).

0272-8842/$36.00
doi:10.1016/j.ceramint.2010.03.014

2. Experimental

$Ba_{0.5}Sr_{0.5}Co_{0.8}Fe_{0.2}O_{3-\delta}$ (BSCF) and $(Ba_{0.5}Sr_{0.5})_{0.8}La_{0.2}CoO_{3-\delta}$ (BSLC) powders were prepared using the citrate–EDTA complexing method. First, 0.08 mole of ethylenediaminetetraacetic acid (EDTA, Riedel-dehaen, 98%) was mixed with 100 ml of 6 M NH_4OH solution to make an NH_3–EDTA solution. Then, 0.016 mole of $Ba(NO_3)_2$ (J. T. Baker, 99.6%) and 0.008 mole of $La(NO_3)_3{\cdot}6H_2O$ (Alfa Aesar, 99.0%) were added, and the mixture was heated and stirred. Next, 0.016 mole of $Sr(NO_3)_2$ (Alfa Aesar, 99.0%) and 0.04 mole of $Co(NO_3)_2{\cdot}6H_2O$ (J. T. Baker, 99.8%) were dissolved in another 100 ml of 6 M NH_4OH solution. These two solutions were mixed and stirred before adding 0.12 mole of citric acid. The resulting mole ratios of EDTA:citric acid:total metal ions were 1:1.5:1. The pH was adjusted to 6 by adding a further 6 M of NH_4OH solution. The final solution was heated to 100 °C on a hotplate and stirred until water evaporated from it, leaving behind a sticky gel. This gel was then heated further at 200 °C for 3 h, calcined at 950 °C for 12 h, and sintered at 1050 °C for 5 h.

The crystal structure of the samples was determined using a powder diffractometer (LabX, XRD-6000) with Ni-filtered Cu Kα radiation; the diffraction angle was ranged from 15° to 85° in 0.01° increments at a rate of 1°/min. The conductivity was measured in air by the DC four-terminal method using Agilent Technologies 34970A and 6645A data acquisition/switch units with silver as the metallic electrode and wire. Thermogravimetry analysis (TGA) was performed from 30 °C to 700 °C at a heating rate of 5 °C/min in air using TA Instruments SDT-Q600 DSC-TGA. The coefficient of thermal expansion (CTE) was measured from 30 °C to 700 °C using a Seiko Instruments TMA/SS 6100 dilatometer with a heating rate of 5 °C/min in air. BSLC–30 wt% $Ce_{0.8}Sm_{0.2}O_{1.9}$ (SDC, Gimat) or BSCF–30 wt% SDC composite films were screen printed on one side of SDC disks to prepare cells for electrochemical impedance spectroscopy (EIS). The SDC substrate disks, 10 mm in diameter and 0.5 mm thick, were prepared by solid-state sintering at 1550 °C for 6 h. A slurry with proper viscosity for screen printing was typically obtained by ball-milling a mixture of 0.3 g BSLC or BSCF powder with 0.13 g SDC powder and 0.0258 g ethyl cellulose-terpineol (J. T. Baker) binder. After screen printing, the cells were baked at 120 °C and then sintered at 1050 °C for 5 h. Pt was used as the reference and counting electrodes on the other side of the electrolyte. The EIS was measured using an impedance analyzer (HIOKI, 3532-50) set to 30 mV over a frequency range from 0.01 Hz to 1 MHz.

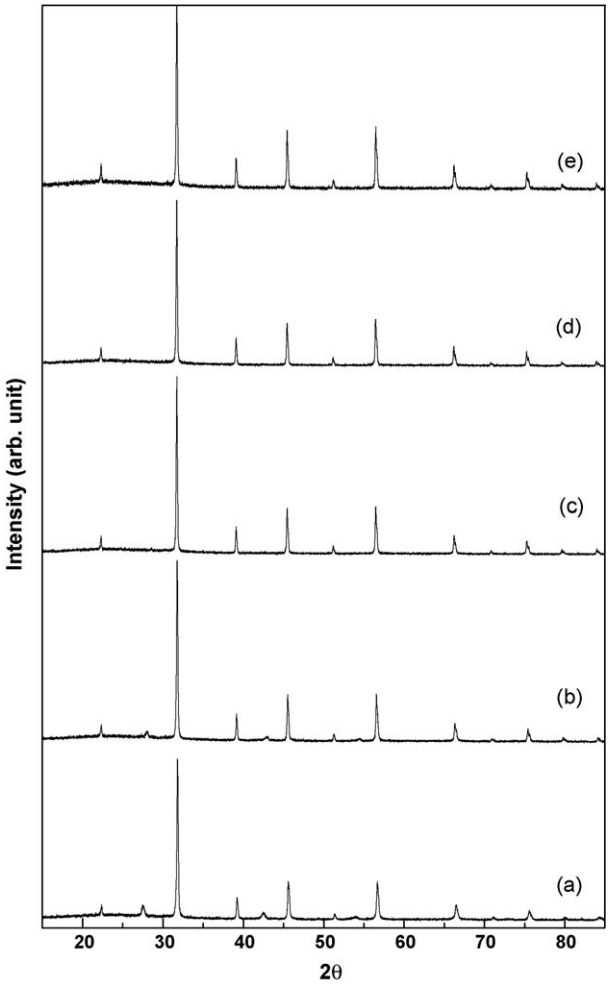

Fig. 1. XRD patterns of BSCF calcined at (a) 850 °C (b) 900 °C, (c) 950 °C, (d) 1000 °C and (e) 1050 °C for 6 h.

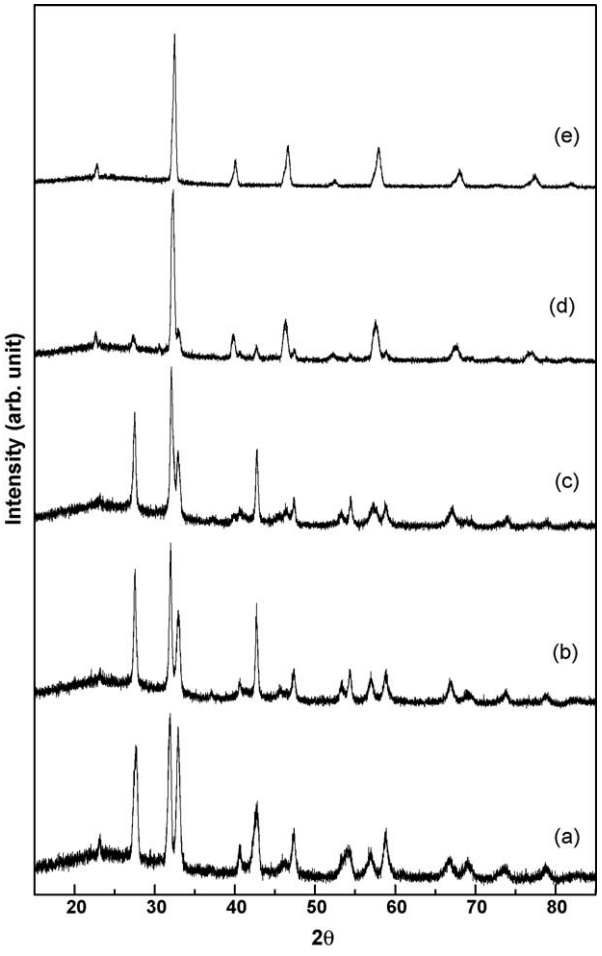

Fig. 2. XRD patterns of BSLC calcined at (a) 850 °C (b) 900 °C, (c) 950 °C, (d) 1000 °C and (e) 1050 °C for 6 h.

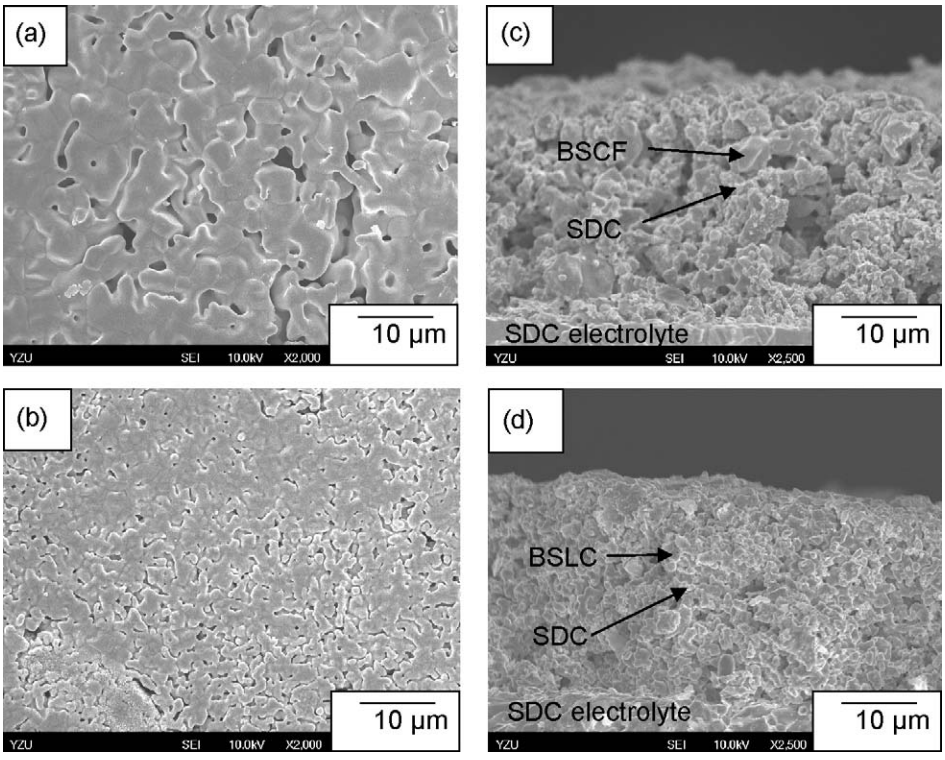

Fig. 3. SEM photographs of (a) BSCF and (b) BSLC and cross-section SEM photographs of (c) BSCF–SDC/SDC and (d) BSLC–SDC/SDC cells showing the electrode–electrolyte interfaces.

3. Results and discussion

Figs. 1 and 2 show the XRD patterns of the BSCF and BSLC powders calcined at various temperatures. Single-phase cubic perovskite BSCF and BSLC (JCPDS 75-0227) were formed at calcination temperatures above 950 °C and 1050 °C, respectively, whereas BSLC has an orthorhombic $BaCoO_{3-\delta}$ structure (JCPDS 47-0211) at calcination temperatures below 950 °C. The structure of BSLC transfers from orthorhombic to cubic at calcination temperatures above 1000 °C. Apparently, the structure transfer temperature of BSLC from orthorhombic to cubic is higher than that of BSCF. For cubic perovskite BSLC and BSCF samples calcined at 1050 °C, the peaks for BSLC was found to shift to the high-angle direction with a lattice parameter a of 3.892 Å, which is much smaller than that of BSCF, 3.987 Å. The substitution of the smaller La^{3+} (0.150 nm) cation instead for the Ba^{2+} (0.175 nm) and Sr^{2+} (0.158 nm) cations is expected to causes lattice shrinkage in BSLC crystals.

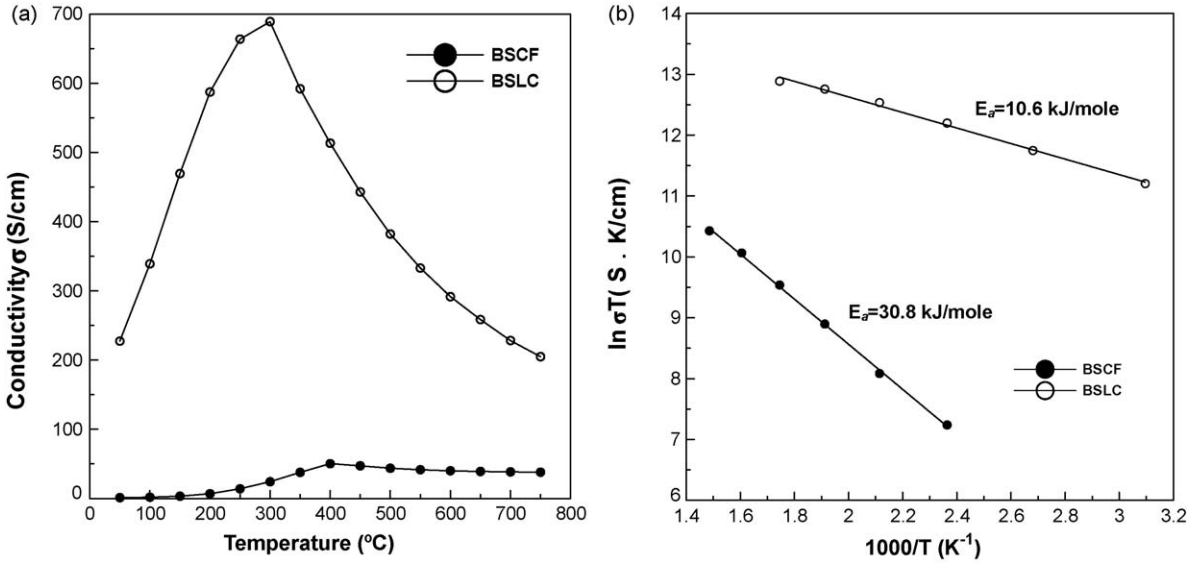

Fig. 4. (a) Conductivity of BSCF and BSLC at different temperatures and (b) Arrhenius plot of the conductivity of BSCF and BSLC.

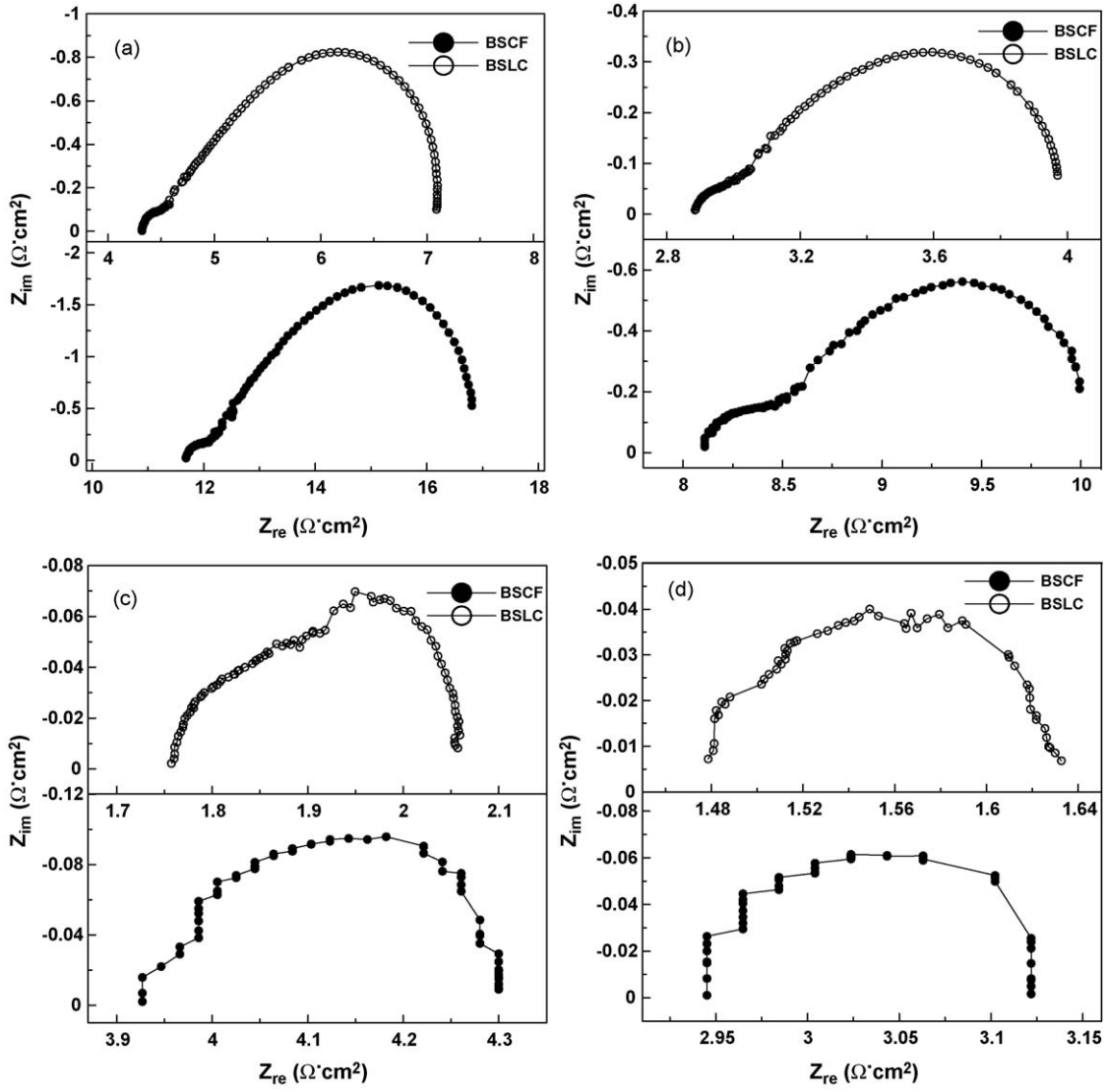

Fig. 5. Impedance spectra of BSCF–SDC and BSLC–SDC composite electrodes. The operating temperature was (a) 600 °C (b) 650 °C (c) 750 °C and (d) 800 °C.

In addition, the ionic radius of Co^{4+} (0.053 nm) is smaller than that of Fe^{4+} (0.0585 nm). Therefore, BSLC is expected to have a smaller lattice parameter than BSCF. The broadness of the XRD peaks of BSLC revealed that BSLC grains are smaller than those of BSCF. Fig. 3 shows the microstructure of the BSCF and BSLC electrodes and the electrode–electrolyte cross-sections of BSCF–SDC/SDC and BSLC–SDC/SDC sintered at 1050 °C for 5 h. The grain size of BSLC is about 1 μm, which is much smaller than that of BSCF (about 10 μm). The thickness of the BSCF–SDC and BSLC–SDC composited electrode was about 20 μm, and no cracks were observed.

Fig. 4(a) shows the conductivity of BSCF and BSLC electrodes as a function of temperature. After an initial increase with rising temperature, the conductivities reach maximum values at 400 °C and 300 °C for BSCF and BSLC, respectively, and then decrease with further increases in temperature. The maximum conductivity of BSLC is 689 S/cm at 300 °C, which is approximately 13 times higher than that of BSCF (50.2 S/cm at 400 °C). The Arrhenius plots in Fig. 4(b) show linear behavior over temperature ranges from 50 °C to ~300/400 °C, for both samples. The gradients in these regions yield activation energies E_a = 30.8 kJ/mole for BSCF and 10.6 kJ/mole for BSLC. The activation energies E_a of BSCF in this study is smaller than that of BSCF reported by Wang [18] and Wei [19]. The activation energy of BSLC is similar to that of BSLCF [17] but much smaller than that of BSSCF [16]. Apparently, the introduction of La^{3+} in A-sites of BSLC improves the conductivity and decreases the activation energy.

Fig. 5 shows the impedance spectra of BSCF–SDC and BSLC–SDC composite electrodes measured at 600–800 °C in air. The equivalent circuit is presented in Fig. 6(a). The elements of the equivalent circuit correspond to electrochemical processes. R_1 corresponds to the resistance of the electrolyte; R_2 corresponds to the resistance of the charge-transfer process. R_3 corresponds to the diffusion resistance of oxygen [15,20,21]. R_2 and R_3 for BSCF–SDC and BSLC–SDC composite electrodes at various temperatures are shown in Fig. 6(b) and (c). The R_2 value of BSLC is much lower than that

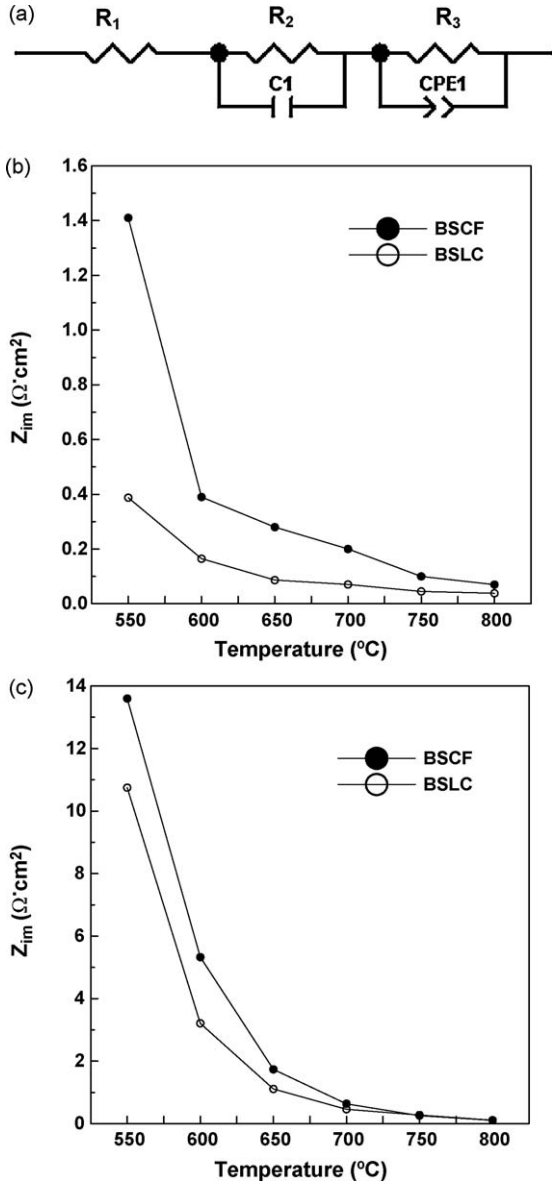

Fig. 6. (a) equivalent circuit for AC impedance spectra and (b) R_2 resistance and (c) R_3 resistance of BSCF–SDC and BSLC–SDC composite electrodes as a function of temperature.

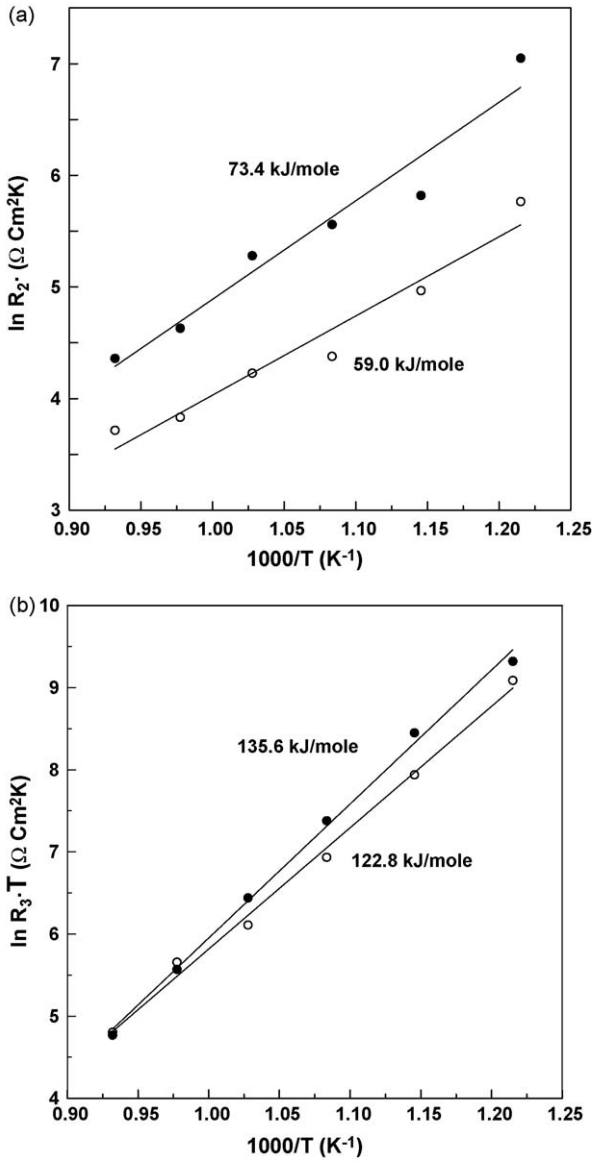

Fig. 7. Arrhenius plots of (a) R_2 resistance and (b) R_3 resistance of BSCF–SDC and BSLC–SDC composite electrodes.

of BSCF, particularly in the low-temperature range of 550 °C to 700 °C. Evidently, the development of a new cathode material by introducing the La^{3+} ion at the A-site results in a significant reduction in charge-transfer resistance. For example, at 550 °C, R_2 = 0.39 Ω cm^2 for BSLC, compared to 1.41 Ω cm^2 for BSCF (representing a 261% reduction) and 1.31 Ω cm^2 for BSSCF (representing a 236% reduction) [16]. The gas-diffusion resistance R_3 of BSLC is a little lower than that of BSCF in the low-temperature range of 550 °C to 650 °C. Fig. 7 shows the Arrhenius plots of R_2 and R_3 over a temperature range from 550 °C to 800 °C. The activation energy for R_2 of BSLC is 50.9 kJ/mole, comparable to that of BSCF (73.4 kJ/mole) and BSLCF15 (78 kJ/mole) [17]. However, the activation energy for R_3 of BSLC shows a large value of 122.8 kJ/mole, which is lower than that for BSCF (135.6 kJ/mole) but much higher than that for BSLCF15 (69.7 kJ/mole) [17].

Although the conductivity mechanism of BSCF-based cathodes is complicated, the concentration of charge carriers in BSCF and BSLC is expected to depend on oxygen valences [23]. Under Po_2 = 0.21 atm, the filling of oxygen vacancies will produce electron holes according to Eq. (1):

$$(1/2)O_{2(g)} + Vo^{\bullet\bullet} \rightarrow O_o{}^x + 2h^{\bullet} \quad (1)$$

The conductivity and TGA data imply that the BSLC samples were p-type conductors below 300 °C in air. The conductivity of this p-type BSLC conductor increases due to hopping between Co^{3+} and Co^{4+}. At temperatures above 300 °C, electrons are produced due to the formation of oxygen vacancies, according to Eq. (2):

$$O_o{}^x \rightarrow Vo^{\bullet\bullet} + 2e' + (1/2)O_{2(g)} \quad (2)$$

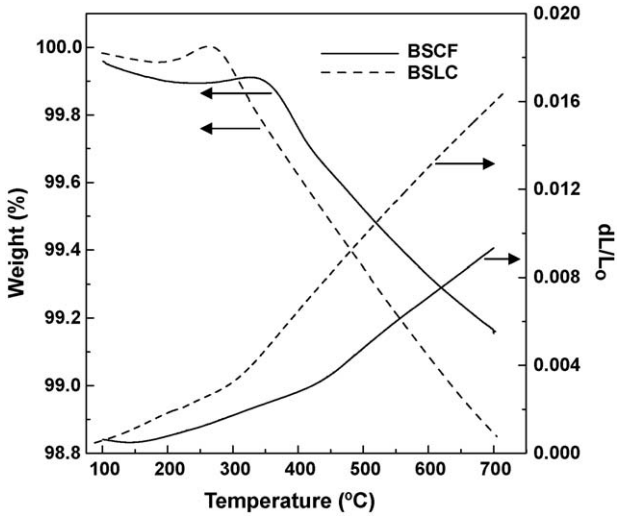

Fig. 8. Thermogravimetry and thermal expansion curves of BSCF and BSLC.

At temperatures above 300 °C, the conductivity of this p-type BSLC conductor decreases with increasing electron concentration due to the formation of oxygen vacancies. It is well known that BSCF-based perovskite tends to lose lattice oxygen on heating [22]. Along with the thermally induced lattice oxygen loss, the reduction of the Co cation to lower states is expected to occur to maintain electrical neutrality, according to Eq. (3):

$$2Co_{Co}^{x} + O_o^{x} \leftrightarrow 2Co_{Co}' + Vo^{\bullet\bullet} + (1/2)O_2 \quad (3)$$

The equilibria given in Eq. (3) will shift to the right with increasing temperature. In addition, the introduction of La^{3+} increases the average valence of A-sites, causing the Co ions to change from IV to III, according Eq. (4):

$$La_2O_3 + 2Co_{Co}^{x} + O_o^{x} \leftrightarrow 2La_{Ba}^{\bullet}(La_{Sr}^{\bullet}) + 2Co_{Co}' + 2O_2 \quad (4)$$

Therefore, the concentration of oxygen vacancies and electron carries increases according Eq. (3). A higher concentration of oxygen vacancies in BSLC samples above 300 °C may be the main reason that the conductivity of BSLC decreases more rapidly than that of BSCF.

Fig. 8 shows the TGA and thermal expansion curves for BSCF and BSLC samples. There is an apparent weight loss above 300 °C and 400 °C for BSLC and BSCF, respectively. These weight losses are due to the loss of lattice oxygen and the formation of oxygen vacancies [22]. Apparently, the weight loss of BSLC (1.14%) is much larger than that of BSCF (0.85%); this suggests that the BSLC electrode has a higher oxygen vacancy concentration. The specific CTE values of BSCF and BSLC are shown in Table 1. The thermal expansion curve of the BSLC sample was linear in the low-temperature range of 50 °C to 300 °C, with a small CTE of $12.2 \times 10^{-6}\,K^{-1}$. A significant inflection occurs above 300 °C, with a high CTE of $31.8 \times 10^{-6}\,K^{-1}$ between 300 °C and 700 °C, due to the loss of lattice oxygen and the formation of oxygen vacancies followed by reduction of Co^{4+} to Co^{3+}. The reduction of $Co^{4+}$to Co^{3+} is associated with an increase in the Co ionic radius. In addition, the reduction of Co^{4+} to Co^{3+} will also decrease the Co–O bond according to Pauling's second rule, resulting in an increase in the size of CoO_6 octahedra, thus enhancing the lattice thermal expansion of BSLC [24]. The CTE of BSLC is $24.2 \times 10^{-6}\,K^{-1}$ from 30 °C to 700 °C, which is a little smaller than that of BSLCF20 ($25.8 \times 10^{-6}\,K^{-1}$) [17] but much larger than that of BSCF ($14.1 \times 10^{-6}\,K^{-1}$). The large thermal expansion of BSLC is due to its higher oxygen vacancy concentration, which was supported by the TGA result.

Table 1
Specific CTE values of BSCF, BSLC, BSLCF and BSSCF.

Sample	CTE ($10^{-6}\,K^{-1}$)		
	30–300*/400 °C	300*/400–700 °C	30–700 °C
BSCF	7.1	21.8	13.7
BSLC	12.2*	31.8*	24.2
BSLCF20 [17]	14.4	31.0	25.8
BSSCF15 [16]	13.1	26.7	20.3

* The CTE data of BSLC divided into two parts: one is between 30 °C to 300 °C and another one is between 300 °C to 700 °C.

These results showed that the BSLC cathode exhibits superior electrical conductivity and excellent electrochemical performance and could be a promising cathode material for IT-SOFCs. However, the CTE value of BSLC is nearly twice that of commercially used SDC electrolytes. This extraordinarily high CTE value could become a major obstacle for BSLC use as a cathode electrode in advanced IT-SOFCs. Preparation of a higher ratio of SDC/BSLC composite cathode electrode is one possible method of overcoming the problem of thermal expansion mismatch. However, the introduction of a high ratio of SDC/BSLC composite cathode may degrade the cathode electrode's performance. The other method is to replace the Co ion by other ions to decrease the CTE of BSLC. In addition, the chemical reaction between BSLC and SDC electrolyte and the performance of a BSLC–SDC composite cathode electrode in a single cell are worthy of future investigation

4. Conclusion

A cubic $(Ba_{0.5}Sr_{0.5})_{0.8}La_{0.2}CoO_{3-\delta}$ perovskite with a small lattice parameter of 3.892 A and grain size of 1 μm was synthesized by the citrate–EDTA complexing method. $(Ba_{0.5}Sr_{0.5})_{0.8}La_{0.2}CoO_{3-\delta}$ showed a maximum conductivity of 689 S/cm at 300 °C and more than 200 S/cm in the operating temperature range of 600–750 °C, which is high enough for use as a cathode electrode in an IT-SOFC. The thermal expansion curve showed an abnormal expansion above 300 °C that was attributed to the loss of lattice oxygen and reduction of Co cations. AC impedance measurements revealed a low charge-transfer resistance of 0.045 Ω cm^2 for $(Ba_{0.5}Sr_{0.5})_{0.8}La_{0.2}CoO_{3-\delta}$–30 wt% $Ce_{0.8}Sm_{0.2}O_{1.9}$ at 750 °C.

Acknowledgements

The authors acknowledge the financial support from the National Science Council in Taiwan under contrast No. NSC

97-2221-E-155-059 and NSC 98-2221-E-155-068. The authors thank Prof. Kuan-Zong Fung (Department of Materials Science and Engineering, National Cheng Kung University) and Prof. Wen-Cheng Wei (Department of Materials Science and Engineering, National Taiwan University) for their kind advice.

References

[1] N.Q. Minh, Ceramic fuel cells, Journal of the American Ceramic Society 76 (1993) 563–588.
[2] P. Leone, A. Lanzini, M. Santarelli, M. Cal, F. Sagnelli, A. Boulanger, A. Scaletta, P. Zitella, Methane free biogas for direct feeding of solid oxide fuel cells, Journal of Power Sources 195 (2010) 239–248.
[3] P. Leone, A. Lanzini, P. Squillari, P. Asinari, M. Santarelli, R. Borchiellini, M. Cal, Experimental evaluation of the operating temperature impact on solid oxide anode supported fuel cells, International Journal of Hydrogen Energy 33 (2008) 3167–3172.
[4] J.B. Goodenough, Y.H. Huang, Alternative anode materials for solid oxide fuel cells, Journal of Power Sources 173 (2007) 1–10.
[5] K.Z. Fung, H.D. Baek, A.V. Virkar, Thermodynamic and kinetic considerations for Bi_2O_3-based electrolytes, Solid State Ionics 52 (1992) 199–211.
[6] V. Gil, J. Tartaj, C. Moure, Chemical and thermomechanical compatibility between Ni-GDC anode and electrolytes based on ceria, Ceramics International 35 (2009) 839–846.
[7] I.M. Hung, H.W. Peng, S.L. Zheng, C.P. Lin, J.S. Wu, Phase stability and conductivity of $Ba_{1-y}Sr_yCe_{1-x}Y_xO_{3-\delta}$ solid oxide fuel cell electrolyte, Journal of Power Sources 193 (2009) 155–159.
[8] A. Moure, A. Castro, J. Tartaj, C. Moure, Mechanosynthesis of perovskite $LaGaO_3$ and its effect on the sintering of ceramics, Ceramics International 35 (2009) 2659–2665.
[9] Q. Xu, D.P. Huang, W. Chen, J.H. Lee, B.H. Kim, H. Wang, R.Z. Yuan, Influence of sintering temperature on microstructure and mixed electronic ionic conduction properties of perovskite type $La_{0.6}Sr_{0.4}Co_{0.8}Fe_{0.2}O_3$ ceramics, Ceramics International 30 (2004) 429–433.
[10] A. Princivalle, E. Djurado, Nanostructured LSM/YSZ composite cathodes for IT-SOFC: a comprehensive microstructural study by electrostatic spray deposition, Solid State Ionics 179 (2008) 1921–1928.
[11] I.M. Hung, K.Z. Fung, C.T. Lin, M.H. Hon, The synthesis and characterization of the $Sm_{0.5}Sr_{0.5}Co_{1-x}Cu_xO_{3-\delta}$ cathode by the glycine-nitrate process, Journal of Power Sources 193 (2009) 116–121.
[12] Z.P. Shao, W.S. Yang, Y. Cong, H. Dong, J. Tong, G.X. Xiong, Investigation of the permeation behavior and stability of a $Ba_{0.5}Sr_{0.5}Co_{0.8}Fe_{0.2}O_3$ oxygen membrane, Journal of Membrane Science 172 (2000) 177–188.
[13] Z. Chen, R. Ran, Z. Shao, H. Yu, J.C.D. Costa, S. Liu, Further performance improvement of $Ba_{0.5}Sr_{0.5}Co_{0.8}Fe_{0.2}O_{3-\delta}$ perovskite membranes for air separation, Ceramics International 35 (2009) 2455–2461.
[14] Z.P. Shao, S.M. Haile, A high performance cathode for the next generation of solid oxide fuel cells, Nature 431 (2004) 170–173.
[15] S. Li, Z. Lu, B. Wei, X. Huang, J. Miao, G. Cao, R. Zhu, W. Su, Electrochemical performance of $(Ba_{0.5}Sr_{0.5})_{0.9}Sm_{0.1}Co_{0.8}Fe_{0.2}O_{3-\delta}$ as an intermediate temperature solid oxide fuel cell cathode, Journal of Power Sources 165 (2007) 97–101.
[16] S. Li, Z. Lu, B. Wei, X. Huang, J. Miao, G. Cao, R. Zhu, W. Su, A study of $(Ba_{0.5}Sr_{0.5})La_{0.2}Sm_xCo_{0.8}Fe_{0.2}O_3$ as a cathode material for IT-SOFCs, Journal of Alloys and Compounds 426 (2006) 408–414.
[17] S. Li, L. Zhe, X. Huang, B. Wei, W. Su, Thermal, electrical, and electrochemical properties of Lanthanum-doped $Ba_{0.5}Sr_{0.5}$ $Co_{0.8}Fe_{0.2}$ $O_{3-\delta}$, Journal of Physics and Chemistry of Solids 68 (2007) 1707–1712.
[18] Y. Wang, S. Wang, Z. Wang, T. Wen, Z. Wen, Performance of $Ba_{0.5}Sr_{0.5}Co_{0.8}Fe_{0.2}O_{3-\delta}$-CGO-Ag cathode for IT-SOFCs, Journal of Alloys and Compounds 428 (2007) 286–289.
[19] B. Wei, L. Zhe, X. Huang, J. Miao, X. Sha, X. Xin, W. Su, Crystal structure, thermal expansion and electrical conductivity of perovskite oxides $Ba_xSr_{1-x}Co_{0.8}Fe_{0.2}O_{3-\delta}$ ($0.3 < x < 0.7$), Journal of the European Ceramic Society 26 (2006) 2827–2832.
[20] F.S. Baumann, J. Fleig, H.U. Habermeier, J. Maier, $Ba_{0.5}Sr_{0.5}Co_{0.8}Fe_{0.2}$ $O_{3-\delta}$ thin film microelectrodes investigated by impedance spectroscopy, Solid State Ionics 177 (2006) 3187–3191.
[21] H.J. Hwang, J.W. Moon, S. Lee, E.A. Lee, Electrochemical performance of LSCF-based composite cathodes for intermediate temperature SOFCs, Journal of Power Sources 145 (2005) 243–248.
[22] J. Ovenstone, J.I. Jung, J.S. White, D.D. Edwards, S.T. Misture, Phase stability of BSCF in low oxygen partial pressures, Journal of Solid State Chemistry 181 (2008) 576–586.
[23] J.I. Jung, S.T. Misture, D.D. Edwards, The electronic conductivity of $Ba_{0.5}Sr_{0.5}Co_xFe_{1-x}O_{3-\delta}$ (BSCF: $x = 0$–1.0) under different oxygen partial pressures, Journal of Electroceramics (in press).
[24] A.L. Shaula, V.V. Kharton, N.P. Vyshatko, E.V. Tsipis, M.V. Patrakeev, F.M.B. Marques, J.R. Frade, Oxygen ionic transport in $SrFe_{1-y}Al_yO_{3-\delta}$ and $Sr_{1-x}Ca_xFe_{0.5}Al_{0.5}O_{3-\delta}$ ceramics, Journal of the European Ceramic Society 25 (2005) 489–499.